

Analysis of the Ratio of (p, pn) to $(p, 2p)$ Reaction Cross Sections

V.B. Shostak¹, G.P. Palkin¹, N.I. Woloshin¹, V.P. Likhachev²,
J.D.T. Arruda-Neto², M.T.F. da Cruz², and M.N. Martins²

¹ *Institute for Nuclear Research, Kiev, Ukraine*

² *Laboratório do Acelerador Linear,
Instituto de Física,
Universidade de São Paulo,
Caixa Postal 66318, 05315-970, São Paulo, SP, Brasil*

Received on 7 November, 2000

The ratio of the differential cross sections for the reactions ${}^7\text{Li}(p, 2p){}^6\text{He}$ and ${}^7\text{Li}(p, pn){}^6\text{Li}$, at incident proton energy of 70 MeV, were analyzed in the framework of DWT approach. FSI and off-shell contributions were factorized and compared with appropriate experimental data.

I Introduction

The quasi-elastic knockout of nucleons by protons, (p, pn) and $(p, 2p)$ reactions, are the source of several, relatively independent pieces of information: reaction mechanism, two-particle forces, interactions in the initial and final states, properties of the states of the residual nuclear systems, and the nuclear wave functions of the knocked out particles.

For initial proton energies (E_o) below ~ 400 MeV, the single-particle character of the proton-nucleon interaction starts to be significantly distorted, even for light nuclei, as a result of various effects. Among them are off-shell effects, when the two-particle scattering is affected by the presence of other particles in the medium. Other kinds of distortion are connected with the interaction of the proton with the nucleus in its initial state (before the quasi-elastic scattering), and with the interaction of the outgoing nucleons with the residual nucleus in the final state (FSI effects). At these energies, the agreement between the calculated and experimental cross sections merely indicates that the wave functions of the intranuclear nucleon, the two-particle potential, and the distortion of the incident proton wave function have been correctly determined.

At $E_o < 100$ MeV, distortion effects are so strong that they determine the character of the reaction. For this reason, the study of knockout reactions induced by protons at these energies deals only with the reaction mechanism and with the correct estimate of the distortions involved.

In Refs. [1-3] various phenomenological nucleon-nucleon potentials were investigated and it was shown

that, while giving a satisfactory description of the free pp scattering, they do not describe adequately the cross sections of $(p, 2p)$ reactions due to off-shell effects. At low to intermediate energies, when the incoming particle energy is of the same order of magnitude of the separation energy, B , of the outgoing particle, the $(p, 2p)$ differential cross sections depend strongly on the off-shell effects present on nucleon-nucleon scattering within the nuclear medium.

Off-shell phenomena are inherent to all many-particle processes, when the scattering in the two-particle system is distorted by other particles in the medium. Only when $B = 0$ and the kinetic energy of the recoil nucleus can be neglected, the relative momenta in the initial and final channels are equal and the two-particle amplitude will be determined on the mass shell.

The off-shell properties of the two-particle amplitude, which could, in principle, be obtained from knockout reactions, can be important in the solution of the inverse problem (deriving the two-particle amplitude from data on nucleon-nucleon scattering). Information about the off-shell behavior of the two-particle amplitude in knockout reactions would eliminate the ambiguity of the problem, since even if a complete set of data on nucleon-nucleon scattering was available, an infinite number of phase-equivalent potentials could be constructed, giving the same two-particle amplitude on the mass shell but differing off it. Unfortunately, off-shell properties are not easy to obtain, since in most experiments it is impossible to disentangle them from other distortion effects.

According to the analysis of Redish [3], $(p, 2p)$

reactions are not sensitive to the off-shell behavior of the two-particle amplitude at energies above 300 MeV. Therefore projectiles above this energy are recommended for the study of the intranuclear nucleon wave functions. For projectile energies below 200 MeV, the $(p, 2p)$ cross section becomes sensitive to the off-shell behavior of the nucleon-nucleon interaction, making this energy region the most convenient for the study of off-shell effects.

In Refs. [4-6] it was shown that usual experimental setups are unable to separate FSI and off-shell effects on the experimental stage. This situation precludes a systematic study of off-shell effects, since it is evidently necessary to separate the distortions and the off-shell effects already at the experiment stage [7]. Nevertheless, as shown in Refs. [8-10], some independent conclusions about the behavior of off-shell and FSI corrections can be drawn from the analysis of the ratio of the cross sections for (p, pn) and $(p, 2p)$ reactions, accomplished in the framework of the distorted-wave approximation for non-local realistic t -matrix (DWTA) approach.

In this work we present an analysis of the ratio of the cross sections for the (p, pn) and $(p, 2p)$ reactions, to show that it is possible to factorize the FSI and off-shell contributions, studying the behavior of each of these contributions versus the separation energy.

II Theoretical Model

The cross section for the ${}^7\text{Li}(p, pn)$ and ${}^7\text{Li}(p, 2p)$ reaction was calculated in the distorted-wave approximation for non-local realistic t -matrix (DWTA). This method was developed by McCarthy and co-workers [11,12] and then improved for the case of arbitrary geometry, eliminating ambiguities in parameters and including an indirect process [13-15]. The indirect process corresponds to the release of an intranuclear nucleon as a result of the interaction of the incident proton with

the residual nucleus [16].

McCarthy abandoned the zero-range approximation and derived a theory of an effective non-local realistic t -matrix suitable for describing the direct $(p, 2p)$ and (p, pn) knockout reactions. The energy-dependent off-shell nucleon-nucleon matrix $t(01, 01; e)$ is an exact solution of the Lippmann-Schwinger equation with a separable nonlocal two-nucleon potential. Here 0, 1, 0, and 1' are generalized coordinates of the nucleons (spatial, spin, and isospin coordinates). A separable non-local potential with a Gaussian form factor was proposed [11] to calculate the radial component of the two-nucleon t -matrix. The corresponding parameters were determined from the phase shifts for elastic p - p and p - n scattering over the energy range 0-350 MeV. The s , p , and d waves were taken into consideration. In the present study we used a similar potential, constructed by Levshin et. al. [17], with a tensor interaction. That potential gives a good description of the energy dependence of the phase shifts when s , p , d , and f waves, in channels with isospins $T = 0$ and 1 and corresponding mixing parameters, are taken into account over the energy range from 0 to 500 MeV. It also describes the singlet and triplet scattering lengths and effective radii. In general, the quantity e , the relative energy of the nucleon-nucleon interaction, has not been defined rigorously for a description of quasielastic processes. In the three-particle problem at hand, the range of this uncertainty is set by a sum of two quantities: the separation energy of the nucleon which is knocked out and the energy of the recoil nucleus.

Having a nonlocal t -matrix, McCarthy included in the matrix element the coordinates of all particles. Then the matrix element for a transition from the initial state i (the system consisting of A nucleons and the incident proton) to the final state f (recoil nucleus and two emitted nucleons) for the mechanism of direct quasifree knockout is

$$T_{fi} = C_{T_f N_f \frac{1}{2} \tau}^{T_i N_i} \sum_m C_{J_f M_f j m}^{J_i M_i} \int [\Psi_{\vec{k}_1}^{(-)}(\vec{r}_0) \Psi_{\vec{k}_2}^{(-)}(\vec{r}_1) S_{\sigma_1}(0) S_{\sigma_2}(0) t_{\tau_1}(1) t_{\tau_2}(1)]^* \times \\ \times t(01, 01; e) \left[\Psi_{\vec{k}_0}^{(+)}(\vec{r}_0' - \frac{\vec{r}_1'}{A}) \right] S_{\sigma_0}(0) t_{\tau_1}(0) \phi_{jm}(1) d\vec{r}_0' d\vec{r}_1' d\vec{r}_0 d\vec{r}_1 \quad (1)$$

Here the subscripts 0, 1, 2 specify the incident particle and the two emitted nucleons, respectively; C are vector-addition coefficients (the first isospin coefficients); S_σ and t_τ are the spin and isospin wave functions of the particles; σ and τ are the projections of the spin and the isospin; j, m, J_f, M_f, J_i and M_i are the angular momenta and respective projections for the

knocked out nucleon, for the core, and for the initial nucleus, respectively.

For convenience in the calculation of multidimensional integrals, McCarthy proposed the use of an analytic form to represent the distorted wave functions (DWF) for the entrance (+) and exit (-) channels, which are used in our calculations. They incorporate

refraction, absorption and focusing, and have an analytical representation similar to the eikonal approximation [13]:

$$\begin{aligned}\Psi_{\vec{k}}^{(+)}(\vec{r}) &= e^{-\gamma \vec{k} R_N} e^{i(\beta+i\gamma)\vec{k}\vec{r}} \left[1 + F e^{-\frac{(\vec{r}-R\vec{k})^2}{S^2}} \right] \\ \Psi_{\vec{k}}^{(-)}(\vec{r}) &= \left[\Psi_{-\vec{k}}^{(+)}(\vec{r}) \right]^*\end{aligned}\quad (2)$$

where $\beta + i\gamma = D$ is the complex refractive index of the optical model. The quantity βk plays the role of a modified wave number, and γ determines the damping. F , R and S are the focusing parameters. R_N is chosen to be equal to the sum of the charge radii of the nucleus and the proton.

In our calculations the DWF parameters were unambiguously chosen from the requirement of: 1) a quantitatively correct description of the experimental data for the elastic (differential and integrated), σ_{el} , reaction, σ_r , and total, σ_{tot} , cross sections for the interaction of the proton (neutron) with the corresponding nuclei in the entrance and exit channels [10] and; 2) agreement between the DWF and the exact wave function, obtained by numerical integration of the Schrödinger equation in a range comparable with the size of the nucleus [14]. Since the experimental results were obtained for two sets of kinematics parameters, corresponding to the following average energies of the final nucleons:

$$\begin{aligned}\langle E_1 \rangle = 22 \text{ MeV} & \begin{cases} \langle E_2 \rangle = 22 \text{ MeV for } 1s \\ \langle E_2 \rangle = 40 \text{ MeV for } 1p \end{cases} \\ \langle E_1 \rangle = 30 \text{ MeV} & \begin{cases} \langle E_2 \rangle = 14 \text{ MeV for } 1s \\ \langle E_2 \rangle = 30 \text{ MeV for } 1p \end{cases}\end{aligned}\quad (3)$$

and the parameters of the DWF were determined for these average energies.

The obtained DWF parameters reproduce the experimental cross sections σ_{el} , σ_r , and σ_{tot} [10] with accuracy better than 10%.

The single-particle bound state wave function ϕ_{jm} was calculated for a Woods-Saxon potential [18], with parameters chosen from the correct description of the binding energies and elastic form factors.

In our case, the effective quasi-two-particle t -matrix is the coherent sum of two terms whose squared moduli determine the cross sections of elastic p - p and p -core scattering [16]. The transition from the matrix $t(01, 01; e)$ to the quasielastic matrix is made by expanding the t -matrix in partial waves and separating the relative and the center of mass coordinates. After this, the 12-fold integral (1) reduces to a 9-fold integral, and it can be calculated analytically by virtue of the exponential representation (expansion with respect to a Gaussian function) and the use of generating functions in the exponential form to calculate the

angular-momentum eigenfunctions. After all the manipulations, all the integrals in (1) become exponentials, the argument of the product of the exponentials being a quadratic form that is transformed to a sum of squares.

III Experimental Procedure

The first study of the ${}^7\text{Li}(p, pn)$ and ${}^7\text{Li}(p, 2p)$ reactions was reported in [10].

The experiment was carried out using the 70-MeV proton beam from the U-240 isochronous cyclotron of the Institute for Nuclear Research of the Ukrainian Academy of Sciences. The experimental facility was described elsewhere [8,10].

Protons and neutrons were detected in coplanar geometry by two spectrometers, located on opposite sides of the initial proton beam trajectory axis. A magnetic spectrometer, based on a two-quadrupole and one-dipole optics, was used for the momentum analysis of the scattered protons, at a fixed angle ($\theta_{p_1} = 45^\circ$) with respect to the initial beam axis. Momentum analyzed protons were detected in the focal plane by an 8-channel scintillation counter with momentum acceptance of 3%.

Energies of the secondary protons (E_{p_2}) and neutrons (E_n) were determined, at definite angles θ_{p_2} , by the time-of-flight spectrometer (TFS). The TFS consisted of five scintillation-counter telescopes, positioned uniformly along a circular arc covering the range $45^\circ - 69^\circ$, in steps of 6° .

The flight paths for protons and neutrons were 3.4 m or 5.7 m. Each telescope consisted of two plastic scintillators (NE102A), 5- and 200-mm thick, respectively, coupled to photomultiplier tubes PM-36. Between the scintillators was placed a lead absorber 8-mm thick to avoid charged particles arriving at the second scintillator. The first scintillator detects practically only protons, since its neutron detection efficiency is very small ($\approx 0.3\%$). The second scintillator detects only neutrons (with about 10% efficiency, see below), since the protons were stopped at the absorber. Signals from the scintillators were used for timing purposes. The energies of the secondary particles were determined from the difference in flight time between them and the scattered protons detected by the magnetic spectrometer. The time resolution, associated mainly with the dimensions of the plastic scintillators, was about 5 ns, producing a 7-8 MeV energy resolution for the detected particles. To keep the background within acceptable levels, the scintillators were shielded by lead and paraffin.

The TDC spectra of pn - and pp -coincidences (time differences between signals from the magnetic and TFS

spectrometers) were recorded by the acquisition system in event-by-event mode. An off-line analysis code allowed the selection of different spectra from the raw data, to calculate the momentum of the recoiling nucleus, k_{A-1} , and the separation energy, B_p or B_n , and rearrange the spectrum versus new variables.

For the analysis presented in this work only events corresponding to symmetric coplanar geometry were chosen: $\theta_1 = \theta_2 = 45^\circ$. These events, for each scattered proton energy, E_m , were arranged in spectra as function of the separation energy.

The pn - and pp -coincidence spectra as function of B_n and B_p , respectively, were decomposed on partial contributions from quasi-free knockout of $1s$ and $1p$ shells. The decomposition was based on a least-squares fit of two Gaussians to the experimental spectra, leaving two free parameters for each peak: height and FWHM. Peak positions were fixed according to the separation energies, obtained in ref. [19] at $E_0 = 1$ GeV.

The differential cross sections for ${}^7Li(p, pn)$ and ${}^7Li(p, 2p)$ reactions, for $1s$ and $1p$ shells, versus (E_p), obtained as a result of the decomposition procedure, are shown in Figs. 1 and 2 by the open circles.

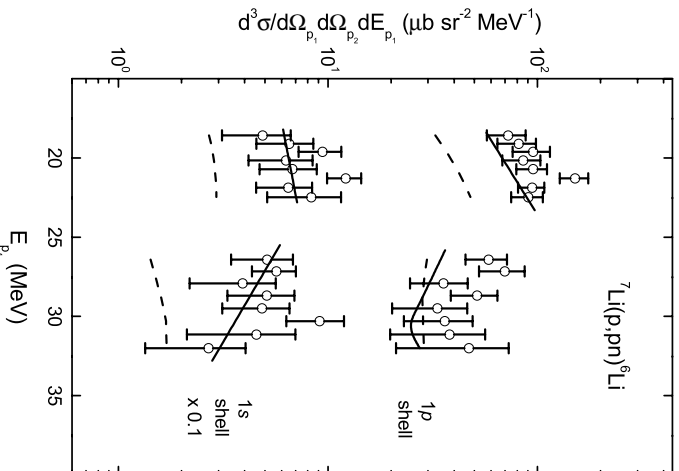


Figure 1. Differential cross sections for the reaction ${}^7Li(p, pn){}^6Li$ at $E_0 = 70$ MeV, for $1p$ and $1s$ shells, versus E_p . Circles represent experimental data from Ref. [10]. Solid curves correspond to a calculation with the DWFA parameters for 6Li in the standard scheme. Dashed curves represent results of the DWFA calculation for a hypothetical FSI, with modified DWFA parameters of 4He (see text for details).

IV Analysis of the ratio of (p, m) to $(p, 2p)$ cross sections

The analysis of the ratio of (p, m) to $(p, 2p)$ cross sections is especially interesting because:

- the ratio of (p, m) to $(p, 2p)$ cross sections, obtained simultaneously and under identical kinematical conditions are free of systematic errors, allowing a direct comparison of these values with other data;
- using this ratio it is possible to separate the FSI and off-shell contributions and to study them independently. Moreover, since the DWFA approach is based on the realistic parameterization of the off-shell and FSI contributions through the use of experimental cross sections, there is no other way to control them in the calculations.

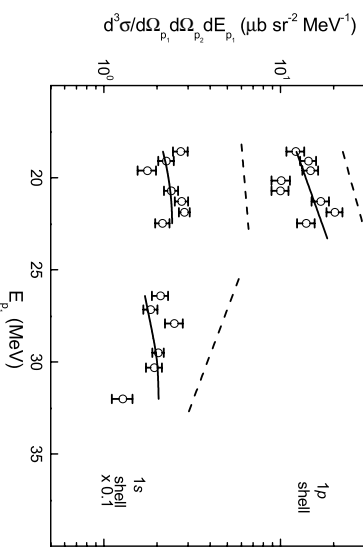


Figure 2. Differential cross sections for the reaction ${}^7Li(p, 2p){}^6He$ at $E_0 = 70$ MeV, for $1s$ and $1p$ shells. Circles represent experimental data from Ref. [10]. Solid curves correspond to calculations with modified DWFA parameters of 4He . The dashed curves represent results of the DWFA calculation for a hypothetical FSI, with parameters of 6Li (see text for details).

As a first step, we define the ratio of the (p, m) to $(p, 2p)$ reaction cross sections, reduced to an equal number of protons, N_p^l , and neutrons, N_n^l , in a given shell, l , and normalized to the elementary proton-neutron, $d\sigma(p, n)$, and proton-proton, $d\sigma(p, p)$, elastic scattering differential cross sections for the same energies and angles, as:

$$\mathfrak{R} = \frac{d^3\sigma(p, pn)^{exp}}{d\sigma(pn)N_n^l} \bigg/ \frac{d^3\sigma(p, 2p)^{exp}}{d\sigma(pp)N_p^l} \quad (4)$$

where $d^3\sigma(p, 2p)^{exp}$ and $d^3\sigma(p, pn)^{exp}$ are the experimental cross sections for the (p, pn) and $(p, 2p)$ reactions, respectively.

In Ref. [19] it was shown that, at sufficiently high E_o , where the impulse approximation is valid, \mathfrak{R} is defined by the single-particle bound state wave functions for protons and neutrons. In the cases where the proton and neutron distributions are identical, $\mathfrak{R} = 1$. Deviations of \mathfrak{R} from unity at high energies are connected with differences between the RMS radii of the nuclear shells for protons (r_{rms}^p) and neutrons (r_{rms}^n) [20,21]. This dependence is strong $\mathfrak{R} \propto \frac{(r_{rms}^n)^4}{(r_{rms}^p)^4}$ [19], and small differences in r_{rms} can result in large deviations of \mathfrak{R} from unity.

Table 1 shows the values of \mathfrak{R} obtained from the data for light nuclei at $E_o = 70$ MeV and 1 GeV, the last values being associated with the single-particle mechanism. At $E_o = 70$ MeV, \mathfrak{R} presents a strong deviation from the single-particle mechanism value. This deviation should be connected with FSI and off-shell effects.

Table I - Experimental values of \mathfrak{R} (see text) for several nuclei at 70 MeV and 1 GeV.

E_o (MeV)		\mathfrak{R}	
Nucleus Shell		70	1000
4He	$1s$	2.1(2) ^b	
6Li	$1p$	3.5(4) ^c	0.95(8) ^d
	$1s$	3.6(4) ^c	1.03(10) ^d
7Li	$1p$	2.3(4) ^c	1.05(4) ^d
	$1s$	2.3(4) ^c	1.08(15) ^d
9Be	$1p^a$	3.9(1.5) ^f	1.58(5) ^d
	$1s$	3.9(1.2) ^f	0.97(12) ^d

^a) $B_n = 18,1$ MeV, ^b) [13], ^c) [22, 23], ^d) [19], ^e) [10], ^f) [8].

In order to separate FSI and off-shell effects in the cross section ratio it is necessary to calculate the $(p, 2p)$ and (p, pn) cross sections with a hypothetical final state interaction ($d^3\sigma(p, 2p)^{hyp}$ and $d^3\sigma(p, pn)^{hyp}$). This is done using, for the DWF in the exit channel, the set of parameters obtained for an isotone of the residual nucleus, instead of the set parameters for the residual nucleus itself, keeping unchanged all another DWTA parameters (off-shell nucleon-nucleon interaction t -matrix, and DWF parameters for the entrance channel).

Then the ratio in eq. (2) could be presented as a product of two factors:

$$\mathfrak{R} = \frac{d^3\sigma(p, pn)^{exp}}{d^3\sigma(p, pn)^{hyp}} \times \frac{d^3\sigma(p, pn)^{hyp} d\sigma(pp)N_p^\ell}{d^3\sigma(p, 2p)^{exp} d\sigma(pn)N_n^\ell} \quad (5)$$

or,

$$\mathfrak{R} = \frac{d^3\sigma(p, 2p)^{hyp}}{d^3\sigma(p, 2p)^{exp}} \times \frac{d^3\sigma(p, pn)^{exp} d\sigma(pp)N_p^\ell}{d^3\sigma(p, 2p)^{hyp} d\sigma(pn)N_n^\ell} \quad (6)$$

The definition of the hypothetical cross sections $d^3\sigma(p, 2p)^{hyp}$ and $d^3\sigma(p, pn)^{hyp}$ implies that the first factors in eqs. (3) and (4), are the ratios:

$$\mathfrak{R}_1^{FSI} = \frac{d^3\sigma(p, pn)^{hyp}}{d^3\sigma(p, pn)^{exp}} \quad (7)$$

and

$$\mathfrak{R}_2^{FSI} = \frac{d^3\sigma(p, 2p)^{hyp}}{d^3\sigma(p, 2p)^{exp}}, \quad (8)$$

which characterize the relative contribution of the distortions caused by FSI effects, since in both ratios $d^3\sigma(p, pn)^{exp}/d^3\sigma(p, pn)^{hyp}$, and $d^3\sigma(p, 2p)^{exp}/d^3\sigma(p, 2p)^{hyp}$, there are no changes connected with possible differences in off-shell effects, but only changes connected with the difference in the exit channels. If FSI effects were negligible (or identical for that pair of isotones) this ratio should be equal to 1. Moreover, directly from the definition of $d^3\sigma(p, 2p)^{hyp}$ and $d^3\sigma(p, pn)^{hyp}$, follows that the ratios:

$$\mathfrak{R}_1^{off-shell} = \frac{d^3\sigma(p, pn)^{hyp} d\sigma(pp)N_p^\ell}{d^3\sigma(p, 2p)^{exp} d\sigma(pn)N_n^\ell} \quad (9)$$

and

$$\mathfrak{R}_2^{off-shell} = \frac{d^3\sigma(p, pn)^{exp} d\sigma(pp)N_p^\ell}{d^3\sigma(p, 2p)^{hyp} d\sigma(pn)N_n^\ell} \quad (10)$$

characterize the relative contribution of off-shell effects only, since in $d^3\sigma(p, pn)^{exp}$ and $d^3\sigma(p, 2p)^{exp}$ we have the same entrance and exit channels as in $d^3\sigma(p, pn)^{hyp}$ and $d^3\sigma(p, 2p)^{hyp}$, respectively, the only change being connected with the difference in off-shell effects due to the difference in the p and n separation energies. If the off-shell effects were negligible (or identical for those isotones) these ratios should be equal to $\frac{(r_{rms}^n)^4}{(r_{rms}^p)^4}$. In particular for the $1p$ and $1s$ shells in 7Li , these ratios should be equal to 1 [19] for $E_o = 1$ GeV (Table 1).

Summarizing, the choice of the hypothetical final states is ruled by the need to separate off-shell and FSI effects. So, if we want to study off-shell effects, we artificially choose a realistic final state of one of the reactions to make the final states of both $(p, 2p)$ and (p, pn) reactions exactly the same, so that the deviations of $\mathfrak{R}^{off-shell}$ from unity will be due to off-shell effects. On the other hand, if we want to study FSI effects, we artificially choose a realistic final state in order to make the same reaction produce different final states, like in eqns. (7) and (8).

Using the experimental and hypothetical cross sections, it was possible to calculate \mathfrak{R}^{FSI} and $\mathfrak{R}^{off-shell}$ for ${}^7Li(p, pn)$, 6Li and ${}^7Li(p, 2p)$, 6He reactions at $E_o = 70$ MeV (Table 2).

Table II - Values of $\mathfrak{R}^{off-shell}$, \mathfrak{R}^{FSI} , and \mathfrak{R} (see text) for several nuclei at 70 MeV.

Nucleus Shell	7Li		4He	9Be	
	$1p$	$1s$	$1s$	$1p$	$1s$
B (MeV)	9	25	21	18	28
$\mathfrak{R}_1^{off-shell} = \frac{(p,pn)^{hyp}(pp)_{\epsilon\ell}N_p^\ell}{(p,2p)^{exp}(pn)_{\epsilon\ell}N_n^\ell}$	1.14(16) ^d	0.68(5) ^d	0.57(5) ^a	-	-
$\mathfrak{R}_2^{off-shell} = \frac{(p,pn)^{exp}(pp)_{\epsilon\ell}N_p^\ell}{(p,2p)^{hyp}(pn)_{\epsilon\ell}N_n^\ell}$	1.15(5) ^c	0.65(7) ^c	0.58(5) ^a	[0.86(8)]	0.68(8) ^b
$\mathfrak{R}_1^{FSI} = \frac{(p,pn)^{exp}}{(p,pn)^{hyp}}$	2.0(1) ^d	3.3(2) ^d	3.6(1) ^a	-	-
$\mathfrak{R}_1^{FSI} = \frac{(p,2p)^{hyp}}{(p,2p)^{exp}}$	1.7(3) ^c	3.1(2) ^c	3.6(1) ^a	3.0(8) ^b	6.0(14) ^b
$\mathfrak{R} = \frac{p,pn)^{exp}(pp)_{\epsilon\ell}N_p^\ell}{p,2p)^{exp}(pn)_{\epsilon\ell}N_n^\ell}$	2.3(4) ^c	2.2(3) ^c	2.1(2) ^a	3.9(15) ^b	3.9(12) ^b
$\mathfrak{R}_1^{FSI} \times \mathfrak{R}_1^{off-shell} = \mathfrak{R}_1^t$	2.3(3)	2.1(2)	2.1(2)	-	-
$\mathfrak{R}_2^{FSI} \times \mathfrak{R}_2^{off-shell} = \mathfrak{R}_1^t$	2.0(3)	2.0(2)	2.1(2)	4.1(12)	3.6(8)

^a) Reference [9,13]. ^b) Reference [2]. ^c) Reference [10,22]. ^d) This work.

V Discussion and conclusions

Results of standard DWTA calculations for the reaction ${}^7Li(p,pn){}^6Li$ are shown in Fig. 1, for both $1s$ and $1p$ shells, by the solid curves, which correspond to the coherent sum of the direct and indirect mechanisms. DWTA calculations quantitatively reproduce the experimental data for both shells within absolute uncertainties ($\sim 15\%$).

For the reaction ${}^7Li(p,2p){}^6He$ it is impossible to carry out the DWTA calculations using the standard calculation scheme used in the case of ${}^4He(p,pn){}^3He$, ${}^4He(p,2p){}^3H$ [13] and ${}^7Li(p,pn){}^6Li$ [10], since the data of elastic and total cross sections for the reactions $(p,{}^6He)$ and $(n,{}^6He)$ do not exist. To circumvent this problem we used a different DWTA calculation scheme, described in [13], and calculated the DWF parameters using the cross sections for a hypothetical residual nucleus (a neighboring stable isotope, for which data exist) and then fitted the focusing parameter R . Using this procedure it was possible to deduce the RMS radius of 8Be [8].

In this calculation scheme, as a first step, we include in the calculation of the differential cross sections for the ${}^7Li(p,2p){}^6He$ reaction the interaction effects of the outgoing nucleons with a hypothetical residual nucleus in the final state (FSI effects) using the cross section of 4He instead of 6He , and then fit the focusing parameter R . The results of such calculations are shown in Fig. 2 by the solid lines. This calculation gives an adequate description of the differential cross sections

for both $1s$ and $1p$ shells, which have different relative contributions from FSI and off-shell effects.

To evaluate the difference in FSI effects when we have 6Li or 6He in the exit channel, we can calculate the ${}^7Li(p,2p)$ cross section with a hypothetical final state interaction, using cross sections for 6Li in the final state, instead for 6He . The results of such calculations are shown in Fig. 2 by the dashed curves. The curves obtained using the hypothetical final state interaction in the calculation present the same shape as, but overestimate the experimental data.

The results of such hypothetical cross section calculations (FSI for 6He instead 6Li) are shown in Fig. 1 by the dashed lines. It is clear that the hypothetical cross section strongly underestimates the experimental results for three of the experimental data sets, reproducing one of them ($1p, E_p \sim 30$ MeV). This situation is expected, since the region around $E_p \sim 30$ MeV corresponds to the minimum of both the momentum transfer and the $1p$ proton cross section [24], and the FSI contribution should fill this minimum, since it tends to increase the cross section around the minimum and to decrease it otherwise. Figures 1 and 2 show that the change from 6Li to 6He in the final state increases the FSI, and, since the RMS radius of 6He is bigger than that of 6Li , and all other DWF parameters are the same, one can conclude that an increase in the RMS radius of the residual nucleus tends to increase the FSI, as it was shown in [19-21]. Note that the DWF is sensitive only to the macroscopic characteristics of the nucleus, like the RMS radius and, as a first approximation, we

could use for the neighboring nuclei the same values of other microscopic parameters, changing only the RMS radius.

Based on the results of the DWTA calculations, which correctly reproduce the experimental ($p, 2p$) and (p, pn) cross sections, we can estimate the order of magnitude of the FSI and off-shell effects in the ratio of these cross sections and study their behavior as a function of the separation energy (Table 2).

Table 2 shows that \mathfrak{R}^{FSI} and $\mathfrak{R}^{off-shell}$, obtained at $E_o = 70$ MeV, significantly differ from those obtained for $E_o = 1$ GeV. This means that the (p, pn) to ($p, 2p$) ratios at $E_o = 70$ MeV contain information about off-shell and FSI effects.

The values obtained for the pairs \mathfrak{R}_1^{FSI} and \mathfrak{R}_2^{FSI} , and $\mathfrak{R}_1^{off-shell}$ and $\mathfrak{R}_2^{off-shell}$, are compatible within uncertainties, although calculated using completely independent experimental cross sections. This suggests that the cross sections are compatible and that the DWTA adequately describes off-shell and FSI effects. In Table 2 only the datum for the $1p$ shell of 9Be corresponds to a case where there is a different spatial distribution of protons and neutrons in the shell ($\rho_p(r) \neq \rho_n(r)$). To keep the compatibility with other calculations, the value of $\mathfrak{R}_2^{off-shell}$ for the $1p$ shell of 9Be was corrected by a factor $(r_{rms}^n)^4 / (r_{rms}^p)^4$ [19], to account for the difference in proton and neutron distributions. The corrected value is presented in Table 2 in square brackets.

$\mathfrak{R}^{off-shell}$ decreases as a function of the separation energy and nuclear number, while \mathfrak{R}^{FSI} presents the opposite tendency. Table 2 also presents products of the ratios: $\mathfrak{R}_1^t = \mathfrak{R}_1^{FSI} \times \mathfrak{R}_1^{off-shell}$ and $\mathfrak{R}_2^t = \mathfrak{R}_2^{FSI} \times \mathfrak{R}_2^{off-shell}$. These products are compatible with the experimental values of \mathfrak{R} . This indicates that, within the achieved accuracy, the contribution of two-stage processes [11,25] are not noticeable in the differential cross sections of ${}^7Li(p, 2p){}^6He$ and ${}^7Li(p, pn){}^6Li$ reactions at $E_o = 70$ MeV.

References

- [1] I.E. McCarthy and K.L. Lim, Phys. Rev. **133**, B1006 (1964).
- [2] I.E. McCarthy and K.L. Lim, Nucl. Phys. **88**, 433 (1966).
- [3] G.J. Stephenson, E.F. Redish, G.M. Lerner, Phys. Rev. C **6**, 1559 (1972); E.F. Redish, G.J. Stephenson, G.M. Lerner, Phys. Rev. C **2**, 1665 (1970).
- [4] L.G. Strobel, Phys. Rev. **C6** (1972) 2039.
- [5] A.I. Vdovin, A.B. Golovin, I.I. Loshchakov, Yad. Fiz. **43**, 1443 (1986); (Sov. J. Nucl. Phys. **43**, 930 (1986)).
- [6] A.I. Vdovin, I.I. Loshchakov, Yad. Fiz. **45**, 67 (1987); (Sov. J. Nucl. Phys. **45**, 42 (1987)).
- [7] A.A. Ioannides, D.F. Jackson, Nucl. Phys. A **308**, 317 (1978).
- [8] V.B. Shostak, G.P. Palkin, N.I. Woloshin, V.P. Likhachev, M.N. Martins, and J.D.T. Arruda-Neto, Phys. Rev. C **61**, 4601 (2000).
- [9] N.I. Woloshin *et al.*, Izv. Acad. Nauk CCCP, ser. fiz. **57**, 218 (1993).
- [10] V.B. Shostak, G.P. Palkin, N.I. Woloshin, V.P. Likhachev, J.D.T. Arruda-Neto, M.T.F. da Cruz, and M.N. Martins, Nucl. Phys. A **643**, 3 (1998).
- [11] P.C. Wright, R.G. Storer and I.E. McCarthy, Phys. Rev. C **17**, 473 (1978).
- [12] R.T. Janus, I.E. McCarthy, Phys. Rev. C **10**, 1041 (1974).
- [13] M.V. Pasechnik *et al.*, Sov. J. Nucl. Phys. **54**, 373 (1991).
- [14] N.I. Woloshin, A.D. Fursa, Ukrainian J. Phys. **39**, 1036 (1994).
- [15] N.I. Woloshin, A.D. Fursa, Ukrainian J. Phys. **40**, 1171 (1995).
- [16] Y. Ikebata, Y. Kudo, Prog. Theor. Phys. **70** (1983) 1457.
- [17] E.B. Levshin *et al.*, Yad. Fiz. **46**, 1614 (1987) (Sov. J. Nucl. Phys. **46**, 961 (1987)).
- [18] L.R.B. Elton and A. Swift, Nucl. Phys. A **94**, 52 (1967).
- [19] C.L. Belostotskii *et al.*, Sov. J. Nucl. Phys. **41** (1985) 903; C.L. Belostotskii *et al.*, Leningrad Institute of Nuclear Physics Report No. 867 (1983).
- [20] H.B. Hakanson *et al.*, Nucl. Phys. A **306**, 406 (1978).
- [21] A.N. James *et al.*, Nucl. Phys. A **324**, 253 (1979).
- [22] M.V. Pasechnik *et al.*, Ukrainian J. Phys. **33**, 976 (1988).
- [23] A.I. Vdovin, *et al.*, Izv. Acad. Nauk CCCP, ser. fiz. **47**, 2219 (1983).
- [24] G. Jacob and T.A. Maris, Rev. Mod. Phys. **38**, (1966) 121; **45**, 6 (1973).
- [25] A.I. Vdovin, A.B. Golovin, I.I. Loshchakov, Sov. J. Nucl. Phys. **42**, 134 (1985).